

KANAZAWA-99-24
 KUCP-0142
 October, 1999

Application of Non-Perturbative Renormalization Group to Nambu-Jona-Lasinio/Gross-Neveu model at Finite Temperature and Chemical Potential

Hiroaki KODAMA^{*)} and Jun-Ichi SUMI ^{*, **)}

*Institute for Theoretical Physics, Kanazawa University, Kakuma-machi,
 Kanazawa 920-1192, Japan*

**Department of Fundamental Sciences, Faculty of Integrated Human
 Studies, Kyoto University, Kyoto 606-8501, Japan*

Abstract

The chiral phase structure of the Nambu-Jona-Lasinio/Gross-Neveu model at finite temperature T and finite chemical potential μ is investigated using (Wilsonian) Non-Perturbative Renormalization Group (NPRG). In the large N_c limit, the solutions of NPRG with various cutoff schemes are shown. For a sufficiently large ultra-violet cutoff, NPRG results coincide with those of Schwinger-Dyson equation and have little cutoff scheme dependence. Next, to improve the approximation, we incorporate the mesonic fluctuations. We introduce the auxiliary fields for mesons, and then derive NPRG equation for finite N_c . The chiral phase structure on (T, μ) plane beyond the leading of $1/N_c$ expansion is investigated in the sharp cutoff limit. N_c dependence of chiral phase diagram is obtained.

^{*)} E-mail address: h-kodama@hep.s.kanazawa-u.ac.jp

^{**) E-mail address: sumi@phys.h.kyoto-u.ac.jp}

§1. Introduction

Explorations of the phase structure of hot/dense QCD or its toy models are of theoretical interest, and it is relevant to the heavy ion experiments planned at RHIC and LHC. At finite temperature and density, the vacuum is expected to move to the quark gluon plasma (QGP) phase via the phase transition, where chiral symmetry is recovered and quarks and gluons are deconfined. Since the phase transition to QGP phase is a non-perturbative phenomenon, we need a non-perturbative analysis to understand it. Unfortunately, there are not so many methods to deal with such problems: lattice Monte Carlo simulation, Schwinger-Dyson equation (SDE), $1/N$ expansion, ϵ expansion. Non-perturbative renormalization group (NPRG) is also one of the methods for such a purpose. The effectiveness of the NPRG method in the non-perturbative phenomena has been investigated by many authors.^{1), 2)}

Non-perturbative renormalization group equations describe the response from the change of infra-red momentum cutoff Λ and can be written down exactly. They are the functional differential equations for the Wilsonian effective action in which the quantum correction from the high energy modes ($p > \Lambda$) are already incorporated. In the practical analysis, we approximate the theory space, the functional space of the effective action, and project the renormalization group equation (RGE) onto this sub-space. By enlarging this sub-space, we can improve the approximations systematically. In some cases, the evaluated physical quantities converge fast under such a process.³⁾ This is an advantageous feature of the NPRG method compared to the asymptotic series, *e.g.* the perturbation theory, ϵ expansion and $1/N$ expansion.

In this article we investigate the chiral phase structure of Nambu-Jona-Lasinio (NJL)/Gross-Neveu (GN) model^{4), 5)} at finite temperature and finite chemical potential. The exploration of the phase diagram is of fundamental interest. If the analysis is extended to QCD, it is of use for the early universe, the astrophysics of neutron stars and the physics of heavy ion collisions. We employ NPRG method for the analyses. It is worth while to examine the applicability of NPRG method, because there does not exist so many other tools for non-perturbative analyses and they do not necessarily work well in any situation.

In lattice Monte Carlo calculation, much exploration has been made in the system at finite temperature,⁶⁾ while the behavior at finite density is much less understood. The non-vanishing chemical potential μ makes fermion determinant to be a complex number, and therefore straightforward Monte Carlo methods can not be applied. At present, two known candidates avoiding this difficulty, *i.e.* Glasgow algorithm⁷⁾ and imaginary chemical potential $\mu = i\nu$ method,⁸⁾ require much larger computer resource but unfortunately do not bring any definite results. Most of the efforts have been done using SDE, but it is difficult

to improve the approximation systematically.

This paper is organized as follows. In §2 we derive the evolution equation which is one of the non-perturbative renormalization group equations and explain local potential approximation (LPA).⁹⁾ In §3 we discuss the chiral phase structure in the large N_c limit, and compare with the results from SDE for the fermion mass function $\Sigma(q)$. Due to the formal equivalence of two methods in the large N_c limit, our large N_c result should coincide with that of SDE. We show consistent results can be obtained in the framework of NPRG method. In §4, we investigate the phase structure beyond the large N_c approximation. Non-perturbative renormalization group method can approximately incorporate the higher order diagrams in $1/N_c$ expansion within local potential approximation. The N_c dependence of the chiral phase diagram will be presented there. §5 is devoted to the summary and discussions.

§2. Evolution equation and local potential approximation

There are three formulations of the non-perturbative renormalization group, the Wegner-Houghton equation, the Polichinski equation and the evolution equation.^{10) - 12)} They are the continuous version of the block spin transformation written in the momentum space and describe the response of lowering the infra-red momentum cutoff Λ . We can find the exact form of renormalization group equation (RGE) for the Wilsonian effective action and/or the effective average action. The latter one is the one particle irreducible part of the Wilsonian effective action. By lowering the cutoff we have the effective action at large distance and incorporate the radiative corrections from the high energy modes. In this article, we employ the evolution equation in Ref.12) and apply to the Nambu-Jona-Lasinio (NJL)/Gross-Neveu (GN) model^{4), 5)} at finite temperature T and chemical potential μ .

The generating functional of connected Green functions is

$$W_\Lambda[\eta, \bar{\eta}] = \ln \int D\bar{\psi} D\psi \exp \left\{ -S_{\text{cut } \Lambda}^f[\bar{\psi}, \psi] - S_{\text{bare}}[\bar{\psi}, \psi] + \bar{\eta} \cdot \psi - \bar{\psi} \cdot \eta \right\}, \quad (2.1)$$

where $S_{\text{cut } \Lambda}^f$ is given by,

$$S_{\text{cut } \Lambda}^f[\bar{\psi}, \psi] = \int_0^{1/kT} d\tau \int d^{d-1}x \bar{\psi} \Delta_f^{-1}(-i\partial, \Lambda) \psi. \quad (*) \quad (2.2)$$

Here Δ_f^{-1} is a cutoff operator and has the property,

$$\Delta_f^{-1}(p, \Lambda) = C^{-1}(p/\Lambda)(p - i\mu\gamma_0) \longrightarrow \begin{cases} 0 & \text{for } p \gg \Lambda \\ \infty & \text{for } p \ll \Lambda. \end{cases} \quad (2.3)$$

^{*)} In the following, we choose units such that Boltzmann constant $k = 1$.

At finite temperature, p_0 is quantized to the Matsubara frequency,

$$\omega_{f,n} = (2n + 1)\pi T \quad \text{or} \quad \omega_{b,n} = 2n\pi T, \quad (2.4)$$

which is for fermions and bosons, respectively. Note that, since $S_{\text{cut } \Lambda}^f$ preserves the chiral symmetry, the effective action also respects it. We choose the cutoff function C as,

$$C^{-1}(p/\Lambda) = \frac{f^2(p/\Lambda)}{1 - f^2(p/\Lambda)}, \quad \text{with} \quad f(p/\Lambda) = \exp[-a(p/\Lambda)^{2b}], \quad (2.5)$$

Since the parameter a can be absorbed in a redefinition of the cutoff Λ , we fix it such that $a = 0.3$ in this paper. The parameter b is the cutoff scheme parameter. ^{*)} Taking the derivative of Eq.(2.1) with respect to Λ and performing the Legendre transformation $\tilde{\Gamma}_\Lambda[\bar{\psi}, \psi] + \bar{\psi} \cdot \Delta_f^{-1} \psi = \bar{\eta} \cdot \psi - \bar{\psi} \cdot \eta - W_\Lambda[\bar{\eta}, \eta]$, we get the evolution equation for the effective average action,

$$\Lambda \frac{d}{d\Lambda} \tilde{\Gamma}_\Lambda[\bar{\psi}, \psi] = -\frac{1}{2} \mathbf{str} \left[\Lambda \frac{d}{d\Lambda} \Delta_f^{-1} \left(\Delta_f^{-1} + \tilde{\Gamma}_\Lambda^{(2)} \right)^{-1} \right], \quad (2.6)$$

where **str** is super-trace which involves momentum (or coordinate) integration, Matsubara summation, spinor summation and color summation. $\tilde{\Gamma}_\Lambda^{(2)}$ is a second (functional) derivative with respect to the fields $\Phi = (\psi^T, \bar{\psi})$ i.e.

$$\left(\tilde{\Gamma}_\Lambda^{(2)} \right)_{xy} \equiv \frac{\overrightarrow{\delta}}{\delta \Phi_x} \tilde{\Gamma}_\Lambda[\Phi] \frac{\overleftarrow{\delta}}{\delta \Phi_y^T}. \quad (2.7)$$

This RGE possesses the exact information about the response of the effective average action to the coarse graining. However, it is a functional differential equation and we can not solve it without approximation. As a first step of our approximation, we neglect higher derivative terms and keep Z factor to be unity. It is called the local potential approximation (LPA). ⁹⁾ This is the leading order of the derivative expansion. ¹³⁾ Since the NPRG preserves

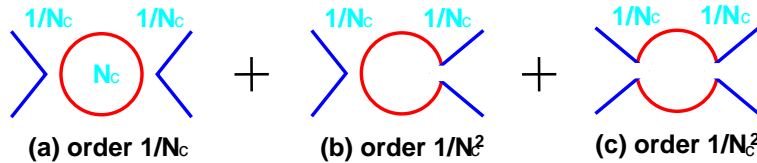


Fig. 1. The Feynman diagrams of four-fermi β functions incorporated in the LPA. The leading contribution in $1/N_c$ expansion corresponds to the first diagram (a). Lines denote the flow of color indices.

the homogeneous global symmetries, the effective average action $\tilde{\Gamma}_\Lambda$ also respects it. So the operator space is restricted to that of the chiral invariants. For example, the independent

^{*)} In § 3, we employ this smooth cutoff regularization to see cutoff scheme b (in)dependence.

chiral invariant four-fermi operators are given as; $\mathcal{O}_1 = (\bar{\psi}\psi)^2 + (\bar{\psi}i\gamma_5\psi)^2$, $\mathcal{O}_2 = (\bar{\psi}\gamma_i\psi)^2 + (\bar{\psi}\gamma_i\gamma_5\psi)^2$ and $\mathcal{O}_3 = (\bar{\psi}\gamma_0\psi)^2 + (\bar{\psi}\gamma_0\gamma_5\psi)^2$ ^{*)}. Here color indices are omitted and i is the spatial index running over $i = 1, 2, 3$. In the LPA, the effective average action is

$$\tilde{I}_\Lambda[\bar{\psi}, \psi] = \int_0^{1/T} d\tau \int d^{d-1}x \left\{ \bar{\psi}(i\partial - i\mu\gamma_0)\psi - \sum_i \frac{G_i}{2N_c} \mathcal{O}_i + \dots \right\}, \quad (2.8)$$

where N_c is the number of colors. In the LPA, the four-fermi operators do not receive any corrections from the multi-fermi operators other than the four-fermi operators. The Feynman diagrams corresponding to the β functions of the four-fermi coupling constants are drown in Fig. 1. In the large N_c limit, the Feynman diagrams (b) and (c) in Fig. 1 don't contribute to our β functions.

§3. Phase structure in the large N_c limit

In this section, we explore the phase structure of the Gross-Neveu model⁵⁾ at finite temperature and chemical potential in the large N_c limit. We attempt to apply the NPRG method to GN model at $T \neq 0$ and $\mu \neq 0$, and show NPRG reproduces consistent results with SDE.¹⁴⁾ In the large N_c limit, only the first diagram (a) in Fig. 1 contributes to the β function of the four-fermi couplings. The β function of the scalar four-fermi coupling $G_s \equiv G_1$ is a function of G_s alone,

$$\frac{d}{dt} \hat{G}_s = -(d-2)\hat{G}_s + 2\hat{G}_s^2 I(a, b; \hat{T}, \hat{\mu}), \quad (3.1)$$

where t is the cutoff scale parameter *i.e.* $\Lambda = \Lambda_0 \exp(-t)$. A profile of the threshold function $I(a, b; \hat{T}, \hat{\mu})$ is given in Appendix A. The characters with hat are the dimensionless coupling constant, *e.g.* $\hat{G}_s = G_s/\Lambda^{d-2}$. The first term of the right hand side (RHS) of Eq.(3.1) corresponds to the canonical scaling and the second one to the radiative correction. At zero temperature and zero chemical potential, we find the two-phase structure by solving the RGE numerically. The RG flow diagram is shown in Fig. 2. There are two phases divided by critical coupling, the strong coupling phase and the weak coupling phase. In the strong coupling phase, the four-fermi coupling constant blows up to the infinity at finite scale t . By evaluating the effective potential of meson fields, we can recognize that the chiral symmetry is spontaneously broken in this phase.²⁾ In the weak coupling phase, the four-fermi coupling goes to zero and chiral symmetry is not broken.

Let us discuss hot and dense matter. The broken chiral symmetry at zero temperature and zero chemical potential is restored at some critical temperature T_c and/or critical chemical

^{*)} We consider only the case with a single flavor.

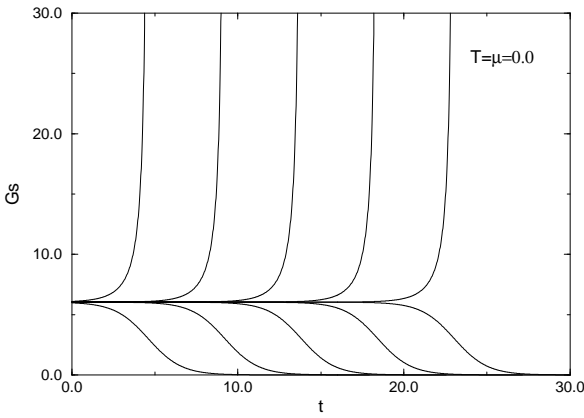


Fig. 2. RG flow diagram for four-fermi coupling \hat{G}_s of three dimensional GN model in the large N_c limit at zero temperature and zero chemical potential. The cutoff scheme is $b = 2.4$.

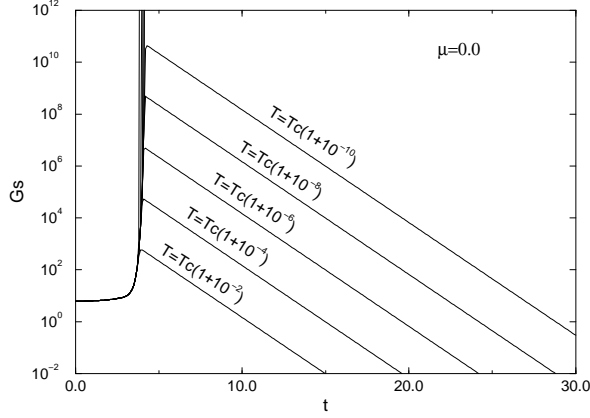


Fig. 3. RG flow diagram for four-fermi coupling \hat{G}_s of three dimensional GN model in the large N_c limit at finite temperature and zero chemical potential. The cut-off scheme is $b = 2.4$.

potential μ_c . We show the RG flow of the four-fermi coupling constant at finite temperature in Fig. 3. There is the critical temperature, below which the four-fermi coupling constant blows up to the infinity. On the other hand, above the critical temperature the four-fermi coupling turns to decrease exponentially.

The temperature/chemical potential dependence of various quantities can be found by solving RGE with the same initial condition as that of $T = \mu = 0$. There are the critical temperature/chemical potential, above which the four-fermi coupling tends to zero, so that chiral symmetry is restored. We can estimate the critical temperature and the critical chemical potential by solving the RG flow equation for the scalar four-fermi coupling constant with some fixed initial condition, or equivalently bare coupling constant. The initial condition should be given at $\Lambda_0 \rightarrow \infty$. However, then we must calculate contributions of infinite number of Matsubara modes since $T/\Lambda = \hat{T}$ goes to zero. ^{*)} In the practical analysis, we solve the RG flow equations with the common initial condition at the sufficiently large but finite ultra-violet cutoff Λ_0 . If Λ_0 is sufficiently large compared with T and μ , the solutions will reach the scaling region where the renormalized information *i.e.* $\Lambda_0 \rightarrow \infty$ limit is obtained. This corresponds to tuning the bare four-fermi coupling constant to the critical one : $\hat{G}_s|_{\Lambda=\Lambda_0} = \hat{G}_s^* + \delta\hat{G}_s$, $\delta\hat{G}_s \rightarrow 0$, where \hat{G}_s^* is the critical coupling constant at

^{*)} As seen from the explicit expression of threshold function in Appendix A, the contributions of high Matsubara modes are suppressed exponentially for a finite \hat{T} . So at some high Matsubara modes, they become to make no contribution within the accuracy of numerical computation. In $\hat{T} \rightarrow 0$ limit, however, infinite number of Matsubara modes contribute.

$T = \mu = 0$. For sufficiently large Λ_0 (or sufficiently small $\delta\hat{G}_s$), the critical temperature and critical chemical potential proportionally depend on the common factor $\delta\hat{G}_s^{-1/(2-d)}$, *i.e.* $T_c(\delta\hat{G}_s) \propto \delta\hat{G}_s^{-1/(2-d)}$, $\mu_c(\delta\hat{G}_s) \propto \delta\hat{G}_s^{-1/(2-d)}$. ^{*)} Thus the ratio of these quantities is independent of the initial value of the four-fermi coupling for the scaling region. The practical problem in the calculations is how large Λ_0 is needed to reach the scaling region. In Figs. 4 and 5, temperature and chemical potential dependence of threshold function I is shown. At small dimensionless temperature $T/\Lambda < 0.03$, threshold functions seem almost

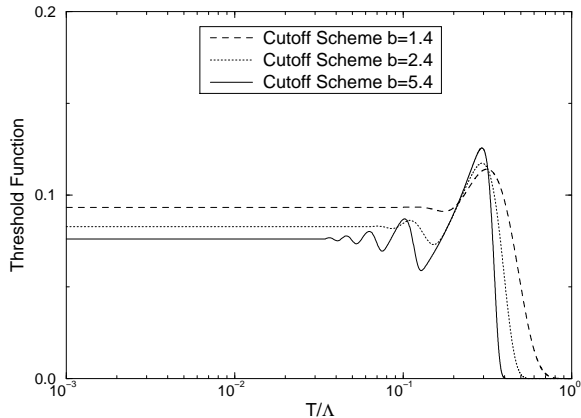


Fig. 4. Temperature dependence of the threshold function I at $\mu = 0$ with various cutoff schemes in three dimensional GN model.

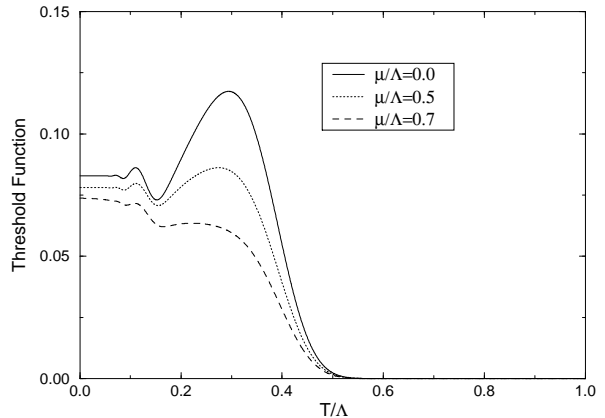


Fig. 5. Temperature dependence of the threshold function I at $\mu \neq 0$ in three dimensional GN model. The cutoff scheme is $b = 2.4$.

constant ^{**) and have almost no temperature dependence. So we expect to reach the scaling region if we set the initial condition at $\Lambda_0 > 33 T$. However, in practice, we must check whether the physical quantities scale correctly or not, since it may depend on the quantities to calculate. We perform the scaling check by calculating a ratio of critical temperature (or chemical potential) and m_0 . Here m_0 is dynamical fermion mass at $T = \mu = 0$.}

We show the results in Fig. 6. If we employ the ultra-violet cutoff $\Lambda_0 = 333 T_{c_0}$, the critical points $(T_c/m_0, \mu_c/m_0)$ almost coincide with those of SDE. Here T_{c_0} is a critical temperature at $\mu = 0$. There is little cutoff scheme dependence using this ultra-violet cutoff Λ_0 . With the ultra-violet cutoff $\Lambda_0 = 333 T_{c_0}$ these quantities reach the scaling region. On the other hand, if we choose the ultra-violet cutoff $\Lambda_0 = 33 T_{c_0}$, the critical points $(T_c/m_0, \mu_c/m_0)$ deviates from those of SDE a little. $\Lambda_0 = 33 T_{c_0}$ is not sufficient to obtain a scaled quantities. We can calculate scaled critical temperature/chemical potential by setting the initial condition at $\Lambda_0 \geq 333 T_{c_0}$. We also plot the results in the sharp cutoff case *i.e.*

^{*)} Other physical quantities, such as the fermion effective mass m_0 at $T = \mu = 0$ also proportionally depend on the factor $\delta\hat{G}_s^{-1/(2-d)}$. For the detailed explanation, see Appendix B.

^{**) They are the values at $T = \mu = 0$.}

$b = \infty$ in Fig. 6. *)

It should be noted that above analyses are based on the flow equation for $1/\hat{G}_s$ rather than Eq.(3.1) for a technical reason. In the large N_c limit, $1/\hat{G}_s$ coincides with the mass squared of the meson fields. Multiplying $-1/\hat{G}_s^2$ to RGE (3.1), it can be rewritten as

$$\frac{d}{dt} \left(\frac{1}{\hat{G}_s} \right) = (d-2) \cdot \frac{1}{\hat{G}_s} - 2I(a, b ; \hat{T}, \hat{\mu}). \quad (3.2)$$

Two phases, chiral broken phase and symmetric phase on (T, μ) plane can be distinguished by the behavior of the solution of eq.(3.2). If $1/\hat{G}_s$ goes to the negative value at sufficiently large t , it is the strong coupling (broken) phase. If $1/\hat{G}_s$ tends to the positive infinity, it is the weak coupling (symmetric) phase. Although Eq.(3.2) and Eq.(3.1) are essentially identical, there emerge difference

on the analyses. If chemical potential $\hat{\mu}$ is large enough, the threshold function I can take negative value. So even if $1/\hat{G}_s$ become negative, $1/\hat{G}_s$ may turn back to the positive value due to the negative I . Thus it should be regarded as weak coupling phase. With RGE Eq.(3.1), this behavior can not be detected because once \hat{G}_s blow up to the infinity, then by mistake we may identify it as the strong coupling phase. Indeed, for a large μ , it gives an inaccurate (about 10%) result. The analysis using $1/\hat{G}_s$ criticality is a more favorable method and we may say, it is a sort of “environmentally friendly renormalization group”.¹⁵⁾

In Ref. 14), the chiral phase structure of GN model in $2 \leq d < 4$ dimensions were calculated using SDE. The effective potentials are calculated in the leading order of the $1/N_c$ expansion. It is known that in $2 \leq d < 3$ chiral phase transition is of first order at low temperature and large chemical potential, and of second order in other region of critical line. In $3 \leq d < 4$, the phase transition is of second order all along the critical line.

Using NPRG we can also derive consistent phase boundaries in any space-time dimen-

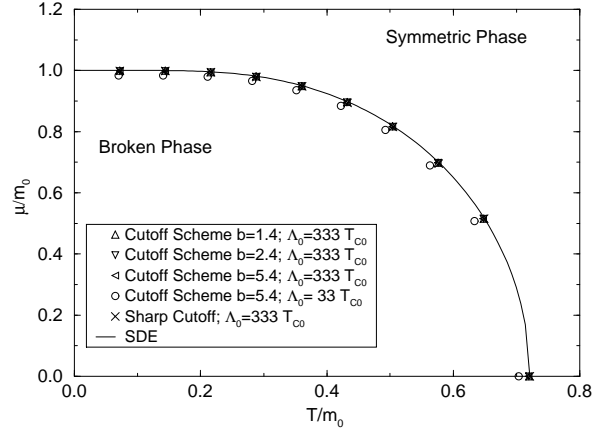


Fig. 6. Chiral phase structure of three dimensional GN model at finite temperature and chemical potential in the large N_c limit. Temperature and chemical potential are normalized by dynamical fermion mass m_0 at $T = \mu = 0$. The dependence of both the cutoff scheme and ultra-violet cutoff Λ in the case of NPRG method Eq. (3.2) and also the results of SDE are shown. The phase transition is of second order all along the critical line.

*) The detailed explanation in the sharp cutoff case is given in § 4.

sions. For example, the chiral phase structure of two dimensional GN model ^{*)} is shown in Fig. 7. In two dimensions, there is the first order critical line as well as the second order one. The phase boundary can be found only by exploring the effective potential V of the collective coordinate σ , which is introduced in the next section. The second order critical point is where $\partial^2 V / \partial \sigma^2|_{\sigma=0} = 0$ is satisfied, while the first order critical point is where the value of the effective potential at the second minimum is equal to that at the first minimum at the origin. The stars in Fig. 7 stands for the first order chiral phase boundary and it terminates at the tricritical point. The filled circles and the open circles are where the signs

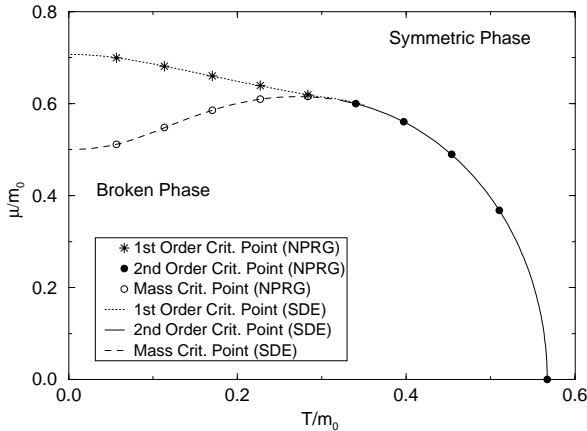


Fig. 7. Chiral phase structure of two dimensional GN model at finite temperature and chemical potential in the large N_C limit. Temperature and chemical potential are normalized by dynamical fermion mass m_0 at $T = \mu = 0$. The symbols are the results using NPRG method. Here cutoff scheme is $b = 1.4$. Ultra-violet cutoff Λ_0 is $333 T_{C0}$. The lines are the results using SDE. Phase boundary consists of the first order critical line and the second order one. The dashed line and the open circles have nothing to do with the phase transition.

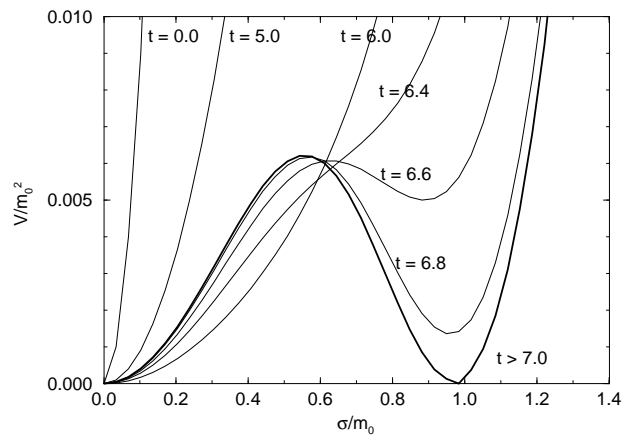


Fig. 8. RG history of the effective potential of two dimensional GN model on the first order phase boundary in the large N_C limit. We choose $T/m_0 = 0.113, \mu/m_0 = 0.682$. The effective potential and the field expectation value are normalized by the dynamical fermion mass m_0 at $T = \mu = 0$. Cutoff scheme here is $b = 1.4$. Ultra-violet cutoff Λ_0 is $333 T_{C0}$.

of meson masses at the origin $\langle \sigma \rangle = 0$ are changed and they correspond to the $1/\hat{G}_s$

^{*)} In two dimensions continuous symmetry can not be spontaneously broken.¹⁶⁾ So we consider the phase transition with a discrete chiral symmetry $\psi \rightarrow \gamma_5 \psi$ in two dimensions.

critical line. The filled circles are identical to the second order chiral phase boundary, but the open circles have nothing to do with the phase transition. The effective potential of two dimensional GN model has a gap structure on the first order phase boundary. An example of the RG evolution of the effective potential at a first order critical point is shown in Fig. 8.

§4. Phase structure beyond the $1/N_C$ leading

In the previous section, we explored chiral phase structure in (T, μ) plane in the large N_C limit. In this section, we improve the approximation beyond the $1/N_C$ leading in four dimensional NJL model. Since we are interested not only in the phase boundary but also in the order of phase transition, the CJT effective potential¹⁷⁾ should be investigated. Let us start from the definition of the partition function,

$$Z_A[J] = \int D\bar{\psi} D\psi \exp \left\{ -S_{\text{cut } A}^f - S_{\text{bare}} + \bar{\eta} \cdot \psi - \bar{\psi} \cdot \eta + \Sigma_\sigma \cdot \bar{\psi} \psi + \Sigma_\pi \cdot \bar{\psi} i\gamma_5 \psi \right\}, \quad (4.1)$$

where $S_{\text{cut } A}^f$, S_{bare} and J are the cutoff action defined in Eq.(2.2), the bare action and the sources $J = \{\eta, \bar{\eta}, \Sigma_\sigma, \Sigma_\pi\}$, respectively. Here the bare action is taken to be,

$$S_{\text{bare}} = \int d^4x \left\{ \bar{\psi}(i\partial - i\mu\gamma_0)\psi - \frac{G_s}{2N_C} [(\bar{\psi}\psi)^2 + (\bar{\psi}i\gamma_5\psi)^2] \right\}. \quad (4.2)$$

We introduce the auxiliary fields σ, π corresponding to the composite operators $\bar{\psi}\psi$, $\bar{\psi}i\gamma_5\psi$ by the following Gaussian integral,

$$\hat{Z}_A = \int D\sigma D\pi e^{-S_{\text{cut } A}^b - \int d^4x \left\{ \frac{1}{2}P^{-1}(\sigma - \Sigma_\sigma - P\bar{\psi}\psi)^2 + \frac{1}{2}P^{-1}(\pi - \Sigma_\pi - P\bar{\psi}i\gamma_5\psi)^2 \right\}}, \quad (4.3)$$

where $S_{\text{cut } A}^b$ is the cutoff action of meson fields and given by,

$$S_{\text{cut } A}^b = \int d^4x \frac{1}{2} (\partial_\mu \sigma C^{-1}(-i\partial/A) \partial_\mu \sigma + \partial_\mu \pi C^{-1}(-i\partial/A) \partial_\mu \pi). \quad (4.4)$$

Here C^{-1} is the cutoff function defined in Eq.(2.5). Note that, since \hat{Z}_A depends on the fields $\bar{\psi}, \psi$ as well as on the sources $\Sigma_\sigma, \Sigma_\pi$, the partition function is deformed by the insertion of \hat{Z}_A except at $A = 0$. Inserting \hat{Z}_A into the path-integral of Eq.(4.1), the partition function becomes

$$\begin{aligned} Z'_A[J] &= \int D\bar{\psi} D\psi D\sigma D\pi e^{-S_{\text{cut } A}^f - S_{\text{cut } A}^b - S_{\text{bare}} + \bar{\eta} \cdot \psi - \bar{\psi} \cdot \eta + P^{-1} \Sigma_\sigma \cdot \sigma + P^{-1} \Sigma_\pi \cdot \pi} \\ &\quad \times e^{-\int d^4x \left\{ \frac{1}{2}P^{-1}(\sigma^2 + \pi^2) - \bar{\psi}(\sigma + \pi i\gamma_5)\psi + \frac{1}{2}P[(\bar{\psi}\psi)^2 + (\bar{\psi}i\gamma_5\psi)^2] + \frac{1}{2P}(\Sigma_\sigma^2 + \Sigma_\pi^2) \right\}} \\ &= \int D\bar{\psi} D\psi e^{-S_{\text{cut } A}^f - S'_{\text{bare}} + \bar{\eta} \cdot \psi - \bar{\psi} \cdot \eta + \Sigma_\sigma \cdot \bar{\psi} \psi + \Sigma_\pi \cdot \bar{\psi} i\gamma_5 \psi}, \end{aligned} \quad (4.5)$$

where S'_{bare} is given by,

$$S'_{\text{bare}} = S_{\text{bare}} - \frac{1}{2} \int d^4x \left\{ (\bar{\psi}\psi + P^{-1}\Sigma_\sigma) [(P^{-1} + C^{-1}\square)^{-1} - P] (\bar{\psi}\psi + P^{-1}\Sigma_\sigma) \right. \\ \left. + (\bar{\psi}i\gamma_5\psi + P^{-1}\Sigma_\pi) [(P^{-1} + C^{-1}\square)^{-1} - P] (\bar{\psi}i\gamma_5\psi + P^{-1}\Sigma_\pi) \right\}. \quad (4.6)$$

In the limit $\Lambda \rightarrow 0$, $Z'_\Lambda = Z_\Lambda$ except for the field independent constant. We modify the generating functional $W_\Lambda[J] = \ln Z'_\Lambda[J]$ as $W'_\Lambda = W_\Lambda + 1/(2P) \cdot (\Sigma_\sigma^2 + \Sigma_\pi^2)$. Physically meaningful quantities are not affected by this modification.¹⁸⁾ Indeed, no vacuum expectation values is changed by adding an arbitrary polynomial of the sources to the generating functional, *e.g.* in our case,

$$\langle \bar{\psi}\psi \rangle = \frac{dW_\Lambda}{d\Sigma_\sigma} \Big|_{\Sigma_{\sigma,\pi}=0} = \frac{dW'_\Lambda}{d\Sigma_\sigma} \Big|_{\Sigma_{\sigma,\pi}=0} - P^{-1}\Sigma_\sigma \Big|_{\Sigma_{\sigma,\pi}=0} = \frac{dW'_\Lambda}{d\Sigma_\sigma} \Big|_{\Sigma_{\sigma,\pi}=0}. \quad (4.7)$$

We rescale the sources as $J' = \{\eta, \bar{\eta}, \Sigma'_\sigma, \Sigma'_\pi\} = \{\eta, \bar{\eta}, P^{-1}\Sigma_\sigma, P^{-1}\Sigma_\pi\}$. The initial condition of RGE at the ultra-violet cutoff $\Lambda = \Lambda_0$ can be given after the Legendre transformation, $\Gamma_\Lambda^{\text{CJT}}[\bar{\psi}, \psi, \sigma, \pi] = \bar{\eta} \cdot \psi - \bar{\psi} \cdot \eta + \Sigma'_\sigma \cdot \sigma + \Sigma'_\pi \cdot \pi - W'_\Lambda[J']$. We have

$$\Gamma_{\Lambda_0}^{\text{CJT}} = S_{\text{bare}} + S_{\text{cut } \Lambda_0}^{\text{f}} + S_{\text{cut } \Lambda_0}^{\text{b}} + \frac{1}{2} \int d^4x P^{-1} \left\{ (\sigma - P\bar{\psi}\psi)^2 + (\pi - P\bar{\psi}i\gamma_5\psi)^2 \right\} \\ = S_{\text{cut } \Lambda_0}^{\text{f+b}} + \int d^4x \left\{ \bar{\psi}(i\partial_0 - i\mu\gamma_0 - \sigma - \pi i\gamma_5)\psi + \frac{N_c}{2G_s}(\sigma^2 + \pi^2) \right\}, \quad (4.8)$$

where $S_{\text{cut } \Lambda}^{\text{f+b}} = S_{\text{cut } \Lambda}^{\text{f}} + S_{\text{cut } \Lambda}^{\text{b}}$. On the last line of Eq.(4.8), we took $P = G_s/N_c$. By subtracting the cutoff action we define the effective averaging action as : $\tilde{\Gamma}_\Lambda[\psi, \bar{\psi}, \sigma, \pi] (= \int d^4x \mathcal{L}_\Lambda) \equiv \Gamma_\Lambda^{\text{CJT}} - S_{\text{cut } \Lambda}^{\text{f+b}}$. In this paper, we approximate it as follows :

$$\mathcal{L}_\Lambda = \bar{\psi}(Z_{f0} i\partial_0 - i\mu)\gamma_0\psi + Z_f \bar{\psi}i\partial_i\gamma_i\psi + \frac{1}{2}N_c Z_{b0}((\partial_0\sigma)^2 + (\partial_0\pi)^2) \\ + \frac{1}{2}N_c Z_b((\partial_i\sigma)^2 + (\partial_i\pi)^2) + y\bar{\psi}(\sigma + i\gamma_5\pi)\psi + N_c V(\sigma^2 + \pi^2). \quad (4.9)$$

There are a yukawa interaction and an effective potential V which is a function of $\sigma^2 + \pi^2$. Here, by a lack of Lorentz symmetry, the wave-function renormalization factors of temporal derivative and those of spatial one are different each other.

The RG flow equation for the effective average action $\tilde{\Gamma}_\Lambda$ can be derived as done in § 2. In our approximation, the RGE becomes a partial differential equation for the effective potential $V(\rho)$ where $\rho = 1/2 \cdot (\sigma^2 + \pi^2)$. If we employ the smooth cutoff function $C(q/\Lambda)$ as done in the previous section, we have to perform the momentum integration with respect to the spatial momenta numerically for each Matsubara modes. It is very time-consuming

and not practical. As investigated in the previous section, the results do not depend on the cutoff scheme for a sufficiently large ultra-violet cutoff Λ_0 at least in the large N_c limit. Therefore it is more promising way to take the sharp cutoff limit of the RG flow equation.¹⁹⁾ After doing so, we need no momentum integration and therefore the computational time is reduced drastically. We can not do Taylor expansion in momentum components p_μ because the sharp cutoff induces non-analyticity at the origin of the momentum space.^{19), 10)} Instead we expand one particle irreducible generating functional $\tilde{\Gamma}_\Lambda$ in momentum scale $|p| = \sqrt{p_\mu p_\mu}$.
*)

In general we may express the cutoff function $C(q/\Lambda)$ as $C^{-1}(q/\Lambda) = 1/\theta_\varepsilon(|q|, \Lambda) - 1$ in terms of $\theta_\varepsilon(|q|, \Lambda)$ which is a smooth regularization of Heaviside θ function of width ε . In the sharp cutoff limit ($\varepsilon \rightarrow 0$), $\theta_\varepsilon(|q|, \Lambda)$ reduces to $\theta(|q| - \Lambda)$ and the evolution equation for the effective average action becomes

$$\frac{d}{d\Lambda} \tilde{\Gamma}_\Lambda[\bar{\psi}, \psi, \sigma, \pi] = -\frac{1}{2} \mathbf{str} \left[\frac{\delta(|q| - \Lambda)}{\gamma(q, \Lambda)} \hat{\Gamma}_\Lambda^{(2)} \left(1 + G \hat{\Gamma}_\Lambda^{(2)} \right)^{-1} \right], \quad (4.10)$$

where we separate the field independent full inverse propagator $\gamma(p, \Lambda)$ from the two point function

$$\left(\tilde{\Gamma}_\Lambda^{(2)}[\bar{\psi}, \psi, \sigma, \pi] \right)_{pp'} = \gamma(p, \Lambda) (2\pi)^4 \delta(p + p') + \left(\hat{\Gamma}_\Lambda^{(2)}[\bar{\psi}, \psi, \sigma, \pi] \right)_{pp'}, \quad (4.11)$$

so that $\hat{\Gamma}_\Lambda^{(2)}[0, 0, 0, 0] = 0$.¹⁹⁾ In Eq. (4.10), $G(p, \Lambda)$ is the infra-red cutoff propagator,

$$G(p, \Lambda) = \lim_{\varepsilon \rightarrow 0} \frac{1}{C^{-1}(p/\Lambda) + \gamma(p, \Lambda)} = \frac{\theta(|p| - \Lambda)}{\gamma(p, \Lambda)}. \quad (4.12)$$

As mentioned above, in the sharp cutoff limit the origin of momentum space is not analytic and Taylor expansion in p_μ breaks down. Alternatively, one should expand in momentum scale. The infra-red cutoff function is expanded in terms of absolute value of external momenta $|p|$ as

$$\theta(|p + q| - \Lambda) = \theta(q \cdot \hat{p} + |p|/2) = \theta(q \cdot \hat{p}) + \sum_{m=1}^{\infty} \frac{1}{m!} \left(\frac{|p|}{2} \right)^m \delta^{(m-1)}(q \cdot \hat{p}). \quad (4.13)$$

Here \hat{p}_μ is a unit vector parallel to p_μ . Integrating RHS of Eq. (4.10) with respect to the internal momenta q , one can expand it in terms of the momentum scale $|p|$. In finite temperature case, the momentum integral in Eq. (4.10) turns to the angular average over three dimensional momenta which are restricted to $\mathbf{q}^2 = \Lambda^2 - \omega_{(b \text{ or } f),n}^2$ for each Matsubara mode. Using the formula of angular integral,

$$\int d^3q \delta \left(|\mathbf{q}| - \sqrt{\Lambda^2 - \omega_{(b \text{ or } f),n}^2} \right) f(\mathbf{q} \cdot \hat{\mathbf{p}}) = 2\pi(\Lambda^2 - \omega_{(b \text{ or } f),n}^2) \int_{-1}^1 dz f(z), \quad (4.14)$$

*) The M th order approximation is to drop all terms beyond $O(|p|^M)$ and the lowest order approximation coincides with the local potential approximation of the Wegner-Houghton equation.¹⁹⁾

we can integrate with respect to the internal momenta \mathbf{q} and expand RHS of RGE (4.10) in terms of the external momenta $|\mathbf{p}|$. The flow equation for the effective potential $V(\rho)$ can be derived. We have

$$\frac{d}{dt}V = \beta_f + \beta_b, \quad (4.15)$$

where β_f is the contribution from fermion loop graphs and β_b is that from boson loop graphs. They are expressed as;

$$\begin{aligned} \beta_f &= -\frac{T}{\pi^2} \sum'_n \zeta_{f,n} \ln \left[1 + \frac{2y^2\rho}{Z_f^2 \Lambda^2 + (Z_{f0}^2 - Z_f^2) \omega_{f,n}^2 - \mu^2 + 2i Z_{f0} \omega_{f,n} \mu} \right], \\ \beta_b &= \frac{T}{4\pi^2 N_C} \sum'_n \zeta_{b,n} \ln \left[Z_b \Lambda^2 + (Z_{b0} - Z_b) \omega_{b,n}^2 + V' \right] \\ &\quad + \frac{T}{4\pi^2 N_C} \sum'_n \zeta_{b,n} \ln \left[Z_b \Lambda^2 + (Z_{b0} - Z_b) \omega_{b,n}^2 + V' + 2\rho V'' \right] \\ &\quad - \frac{T}{4\pi^2 N_C} \sum'_n \zeta_{b,n} \ln \left[Z_b \Lambda^2 + (Z_{b0} - Z_b) \omega_{b,n}^2 + V' \right]^2 \Big|_{\rho=0}. \end{aligned} \quad (4.16)$$

where $\zeta_{(b \text{ or } f),n} = \sqrt{\Lambda^2 - \omega_{(b \text{ or } f),n}^2} \cdot \Lambda^2$ and the prime ' operating on the effective potential V denotes the derivative with respect to ρ . \sum'_n is the summation about n with the condition $\omega_{(b \text{ or } f),n}^2 \leq \Lambda^2$. For the wave function renormalization factor Z_b , we have ^{*)}

$$\begin{aligned} \frac{d}{dt}Z_b &= \frac{2T}{\pi^2} \sum'_n \frac{\zeta_{f,n} Z_f^2 y^2}{(Z_f^2 \Lambda^2 + (Z_{f0}^2 - Z_f^2) \omega_{f,n}^2 - \mu^2 - 2i Z_{f0} \mu \omega_{f,n})^2} \\ &\quad \cdot \left(\frac{1}{2} - \frac{1}{3} \frac{Z_f^2 (\Lambda^2 - \omega_{f,n}^2)}{Z_f^2 \Lambda^2 + (Z_{f0}^2 - Z_f^2) \omega_{f,n}^2 - \mu^2 - 2i Z_{f0} \mu \omega_{f,n}} \right). \end{aligned} \quad (4.17)$$

In this paper, we also approximate Z_{b0} as $Z_{b0} = Z_b$. In the large N_C limit, the boson fluctuations disappeared, *i.e.*, $\beta_b = 0$ due to a factor $1/N_C$. However for finite N_C , we must incorporate the boson loop contributions, β_b . This is a significant difference from the large N_C limit. In general the fermion contribution makes the effective potential evolve downward as cutoff is lowered, while the boson contribution lifts the effective potential upward. ^{**) The latter is main additional effect for finite N_C on the RG evolution of the effective potential and hence also on the chiral phase structure on (T, μ) plane. We shall ignore the corrections to fermion's Z factors Z_f , Z_{f0} and to yukawa coupling y ^{***)} as the first step toward the}

^{*)} In momentum scale expansion of sharp cutoff effective average action, there emerges a kinetic term proportional to $|\mathbf{p}|$. The non-analytic dependence on momenta at $\mathbf{p} = 0$ lead to a non-locality in position space. Since the resulting physics in the limit $\Lambda \rightarrow 0$ should not suffer from this non-locality, it should be absorbed by a certain counter term. Here we simply neglect it in our approximation.

^{**) This is understood from the signs of β_f and β_b .}

^{***)} Here, we do not renormalize the boson fields σ, π to make their Z factor unity, *i.e.* $Z_b = 1$, since at ultra-violet cutoff, it should vanish. Therefore in an ordinary sense, our physical yukawa coupling runs due to bosonic wave-function renormalization.

exploration of the phase structure at finite temperature and finite chemical potential beyond the $1/N_C$ leading. ^{*)}

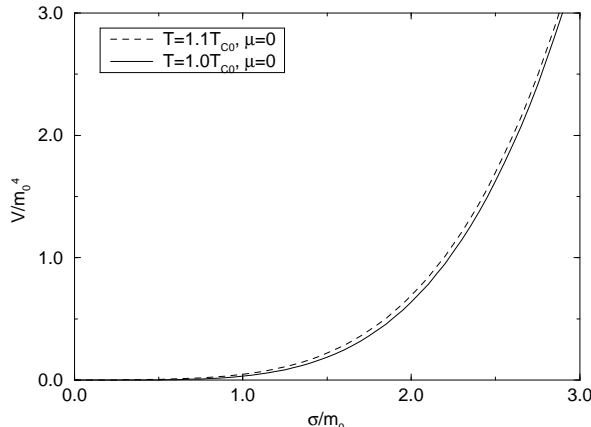


Fig. 9. The effective potential of four dimensional NJL model at finite temperature. Here, $N_C = 10$. The effective potential and the field expectation value are normalized by the dynamical fermion mass m_0 at $T = \mu = 0$.

σ , it is a broken phase. If the temperature (or the chemical potential) is greater than the critical one, the effective potential has a minimum at the origin, *i.e.* the chiral symmetry is recovered. If the temperature (or the chemical potential) is below the critical one, the effective potential has a nontrivial minimum. More precisely, in the broken phase, the effective potential evolves toward the so-called ‘convex’ one.^{25), 26)} Some results of the effective potentials are shown in Fig. 9.

Table I. The critical temperature T_{c0} and the chemical potential μ_{c0} of the four dimensional NJL model.

| N_C | 10 | 20 | 40 | 80 | ∞ |
|-------------------|------|------|------|------|----------|
| T_{c0}/m_0 | 1.07 | 1.21 | 1.30 | 1.35 | 1.38 |
| μ_{c0}/m_0 | 2.58 | 2.70 | 2.81 | 2.83 | 2.83 |
| μ_{c0}/T_{c0} | 2.41 | 2.23 | 2.16 | 2.10 | 2.05 |

Taking into account of the discussions in the previous section, we take an initial condition of RG flow equations at $\Lambda_0 = 333 T_{c0}$. Indeed, with this condition, the critical line almost coincided with that from SDE in three dimensional GN model for $N_C = \infty$ (See Fig. 6).

^{*)} A similar approximation is performed in Ref. 20).

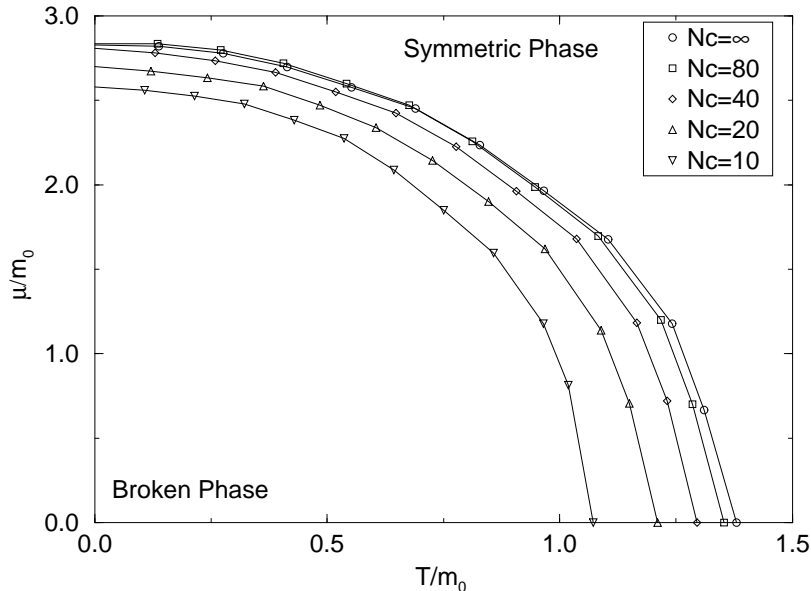


Fig. 10. N_c dependence of the chiral phase structure of the four dimensional NJL model at finite temperature and chemical potential. In each N_c , the phase transition is of second order or very weak first order all along the critical line. The temperature and the chemical potential are normalized by the dynamical fermion mass m_0 at $T = \mu = 0$.

The chiral phase diagram on (T, μ) plane is shown in Fig. 10. Here, the temperature and the chemical potential are normalized by the dynamical fermion mass $m_0 = y < \sigma >$ at zero temperature and zero chemical potential. In each N_c case, the phase transition is found to be of second order or very weak first order all along the critical line from the shape of the effective potentials at the critical points. For example, an effective potential at a critical point for $N_c = 10$ is shown in Fig. 9. N_c dependence of the critical line on (T, μ) plane is not small. The critical temperature and the critical chemical potential become small in unit of m_0 if N_c is lowered. This is due to the boson fluctuations existing for finite N_c . Intuitively, we can understand it as follows. The fermionic negative corrections (β_f) to the effective potential are suppressed by a high temperature and/or a large chemical potential, but the bosonic positive ones (β_b) are less suppressed due to the existence of Matsubara zero mode. Hence if the bosonic part becomes large, that is, the case of small N_c , the chiral symmetry is restored at lower temperature (smaller chemical potential) in comparison with the large N_c case. N_c dependence of the critical temperature at $\mu = 0$ (T_{c0}) as well as that of the critical chemical potential at $T = 0$ (μ_{c0}) are shown in Table I. *)

*) The numerical calculations for $N_c < 10$ need much finer mesh in t direction because β_b becomes large. This will be a subject in the forthcoming paper.

§5. Summary and discussion

We performed a non-perturbative analysis by the (Wilsonian) non-perturbative renormalization group in NJL/GN model at finite temperature and chemical potential and explored chiral phase structure on (T, μ) plane.

First we explored the phase structure of the GN model at finite temperature and chemical potential in the large N_c limit. We showed that consistent results with those of SDE could be obtained in the framework of NPRG method. We investigated how large ultra-violet cutoff Λ_0 is needed to obtain scaled quantities. We could calculate scaled critical temperature/chemical potential by setting the initial condition at $\Lambda_0 = 333 T_{c0}$ and they had little cutoff scheme dependence.

Second we improved the approximation beyond the $1/N_c$ leading in four dimensional NJL model. For finite N_c , the bosonic fluctuations have to be incorporated. In § 4, we introduced the mesonic auxiliary fields σ, π , and derived the flow equation for the effective potential of these fields $V(\sigma^2 + \pi^2)$. RG flow equation is then a non-linear partial differential equation for this potential. Taking account of the possibility of the first order phase transition like Fig.8 and the cubic term $\rho^{3/2}$,²¹⁾ we solved the partial differential equation for $V(\sigma^2 + \pi^2)$ without a polynomial expansion employed in Ref.3). For several N_c , we obtained the chiral phase structure on (T, μ) plane. For $N_c = 10 \sim \infty$, the phase transition is second order or very weak first order all along the critical line. The critical temperatures/chemical potentials depend on N_c largely, and become small as N_c is decreased. For $N_c = 10$, T_{c0} is 78% of that for $N_c = \infty$.

Generalization of this analysis to more realistic models, QCD seems to be straightforward, except for the treatment of the gauge invariance. By introducing the instanton induced multi-fermi operator,²⁴⁾ NPRG method can be also applied to the color-superconductor.²⁷⁾

Acknowledgments

We would like to thank W.Souma for informative discussions on numerical computation, and K-I.Aoki, T.Suzuki, and H.Terao for useful comments. Part of numerical computations in this work were carried out in the Yukawa Institute Computer Facility.

Appendix A

— *Threshold functions* —

In this appendix we show the explicit form of the threshold functions $I(a, b ; \hat{T}, \hat{\mu})$ appeared in Eq.(3.1). In d dimensions, the threshold function at zero temperature and zero

chemical potential is

$$I(a, b ; 0, 0) = \frac{1}{2^{d-1} \pi^{d/2} \Gamma(d/2)} \int_0^\infty dq q^{d-3} 2^{(d/2+2)} a b q^{2b} (1 - f^2(q)) f^2(q). \quad (\text{A.1})$$

For finite temperature and/or chemical potential, the threshold function can be obtained by the replacement $\int dq^d/(2\pi)^d \rightarrow \hat{T} \sum_n \int dq^{d-1}/(2\pi)^{d-1}$ and $q_0 \rightarrow \hat{\omega}_{f,n} - i\hat{\mu} = (2n+1)\pi\hat{T} - i\hat{\mu}$,

$$I(a, b ; \hat{T}, \hat{\mu}) = \frac{1}{2^{d-2} \pi^{(d-1)/2} \Gamma((d-1)/2)} \hat{T} \sum_{n=0}^\infty \int_0^\infty dq q^{d-2} 2^{(d-1)/2+3} a b (\hat{\omega}_{f,n}^2 + q^2)^b (1 - f^2(q)) f^2(q) \frac{\hat{\omega}_{f,n}^2 - \hat{\mu}^2 + q^2}{\{\hat{\omega}_{f,n}^2 + (q + \hat{\mu})^2\} \{\hat{\omega}_{f,n}^2 + (q - \hat{\mu})^2\}}. \quad (\text{A.2})$$

$\hat{T} \rightarrow 0$ and $\hat{\mu} \rightarrow 0$ limit of Eq.(A.2) coincides with Eq.(A.1).

Appendix B

— Renormalization and the continuum limit at $T, \mu \neq 0$ —

Let us discuss renormalization and the continuum limit at finite temperature and finite chemical potential in this appendix. In the large N_c limit, the RG β functions are given by,

$$\frac{d}{dt} \hat{G}_s = -(d-2) \hat{G}_s + I(\hat{T}, \hat{\mu}) \hat{G}_s^2, \quad (\text{B.1})$$

$$\frac{d}{dt} \hat{T} = \hat{T}, \quad (\text{B.2})$$

$$\frac{d}{dt} \hat{\mu} = \hat{\mu}. \quad (\text{B.3})$$

Fixed points of the above RG equations at $\hat{T} = \hat{\mu} = 0$ are the Gaussian fixed point $\hat{G}_s = 0$ and Gross-Neveu point $\hat{G}_s = (d-2)/I(\hat{T} = 0, \hat{\mu} = 0) \equiv \hat{G}_s^*$. Note that, $\hat{T} = \infty$ and/or $\hat{\mu} = \infty$ are also fixed points. If $\hat{T} = \infty$ and/or $\hat{\mu} = \infty$ then only Gaussian fixed point can be found for the finite \hat{G}_s , since $I(\hat{T}, \hat{\mu})$ vanishes. The difference from an ordinary zero temperature and zero chemical potential field theory is $\hat{T}, \hat{\mu}$ dependence of the threshold function I . As will be explained below, it does not affect the ‘renormalization’.

We linearize the RG equations around the GN point. ^{*)} Letting $\hat{G}_s = \hat{G}_s^* + \delta\hat{G}_s$, we have,

$$\frac{d}{dt} \delta\hat{G}_s = -(d-2) \delta\hat{G}_s + 2I_0 \hat{G}_s^* \delta\hat{G}_s + (\hat{T} I_0^T + \hat{\mu} I_0^\mu) \hat{G}_s^{*2} \quad (\text{B.4})$$

$$\frac{d}{dt} \hat{T} = \hat{T}, \quad (\text{B.5})$$

$$\frac{d}{dt} \hat{\mu} = \hat{\mu}, \quad (\text{B.6})$$

^{*)} For the infinitesimal neighborhood of the fixed point, this linearization is valid.

where $I_0 = I(\hat{T} = 0, \hat{\mu} = 0)$, $I_0^T = (\partial I / \partial \hat{T})(\hat{T} = 0, \hat{\mu} = 0)$ and $I_0^\mu = (\partial I / \partial \hat{\mu})(\hat{T} = 0, \hat{\mu} = 0)$. By Lorentz symmetry at $\hat{T} = \hat{\mu} = 0$, $I_0^\mu = 0$. We also find $I_0^T = 0$, since the difference between $I(\hat{T}, 0)$ and I_0 is $\mathcal{O}(\hat{T}^2)$. ^{*)} Consequently, we find,

$$\frac{d}{dt} \begin{pmatrix} \delta \hat{G}_s \\ \hat{T} \\ \hat{\mu} \end{pmatrix} = \begin{pmatrix} -(d-2) + 2I_0 \hat{G}_s^* & \mathbf{0} \\ & 1 \\ \mathbf{0} & 1 \end{pmatrix} \begin{pmatrix} \delta \hat{G}_s \\ \hat{T} \\ \hat{\mu} \end{pmatrix}. \quad (\text{B.7})$$

The eigenvalues are found to be $\nu_1 = d-2$, $\nu_2 = \nu_3 = 1$. Here we used $\hat{G}_s^* = (d-2)/I_0$. We derive the relations between the bare coupling and the physical quantities using an ordinary procedure. Let us focus on the infinitesimal neighborhood of GN point, *i.e.* we consider the continuum limit of the theory $\Lambda_0 \rightarrow \infty$. The critical temperature T_c is completely determined by mutually independent three variables: the bare four-fermi coupling $\delta \hat{G}_s$, bare chemical potential $\hat{\mu}_0$ and the ultra-violet cutoff Λ_0 . The extra $\hat{\mu}_0$ dependence of the critical temperature *i.e.* $T_c(\delta \hat{G}_s, \Lambda_0; \hat{\mu}_0)$ does not affect to the following considerations. Now it is convenient to think that the critical temperature depends on the ‘bare’ chemical potential $\hat{\mu}_0$ through the fixed as well as RG invariant dimensionless ratio $\hat{\mu}_0/\hat{T}_0$. As everyone knows, the RG preserves the physical quantities. Therefore, we can realize by solving the RG equations from Λ_0 to $\Lambda = \lambda \Lambda_0$ that the critical temperature satisfies,

$$T_c(\delta \hat{G}_s, \Lambda_0; \hat{\mu}_0/\hat{T}_0) = T_c(\lambda^{-(d-2)} \delta \hat{G}_s, \lambda \Lambda_0; \hat{\mu}_0/\hat{T}_0), \quad (\text{B.8})$$

where we used the solution,

$$\delta \hat{G}_s = C e^{(d-2)t} = C(\Lambda_0/\Lambda)^{d-2}. \quad (\text{B.9})$$

Here C is the ‘bare’ $\delta \hat{G}_s(\Lambda_0)$. The relation (B.8) can be rewritten by the dimensionless critical temperature $\hat{T}_c(\delta \hat{G}_s; \hat{\mu}_0/\hat{T}_0) = T_c(\delta \hat{G}_s, \Lambda_0; \hat{\mu}_0/\hat{T}_0)/\Lambda_0$ ^{**) as}

$$\hat{T}_c(\delta \hat{G}_s; \hat{\mu}_0/\hat{T}_0) = \lambda \hat{T}_c(\lambda^{-(d-2)} \delta \hat{G}_s; \hat{\mu}_0/\hat{T}_0). \quad (\text{B.10})$$

Hence,

$$\hat{T}_c(\delta \hat{G}_s; \hat{\mu}_0/\hat{T}_0) \propto \delta \hat{G}_s^{1/(d-2)}. \quad (\text{B.11})$$

If one starts from the temperature dependent critical chemical potential, then one finds,

$$\hat{\mu}_c(\delta \hat{G}_s; \hat{\mu}_0/\hat{T}_0) \propto \delta \hat{G}_s^{1/(d-2)}. \quad (\text{B.12})$$

^{*)} $I(\hat{T}, 0)$ is like an approximation of the integral I_0 by a histogram, band width of which is $2\pi\hat{T}$. As a trapezoidal rule estimate differs from an integral by an order of the square of the width,²²⁾ $I(\hat{T}, 0)$ also differs from I_0 by $\mathcal{O}(\hat{T}^2)$.

^{**)} By dimensional analysis, \hat{T}_c is independent of Λ_0 .

One can also find a similar relation of the fermion dynamical mass at $T = \mu = 0$, $m_0 \propto \delta \hat{G}_s^{1/(d-2)}$. We can ‘renormalize’ these quantities by taking $\delta \hat{G}_s(\Lambda_0) = (M/\Lambda_0)^{(d-2)}$, where M is some finite reference mass scale. Letting $\Lambda_0 \rightarrow \infty$, we find the continuum limit of GN model at finite temperature and/or finite chemical potential.

The above observations can be straightforwardly generalized to other models.

References

- 1) U. Ellwanger and C. Wetterich, Nucl. Phys. **B423** (1994), 137.
D.U. Jungnickel and C. Wetterich, Phys. Rev. **D53** (1996), 5142; Eur. Phys. J. **C1** (1998), 669; **C2** (1998), 557; Phys. Lett. **B389** (1996), 600; Heidelberg preprints HD-THEP-96-40, [hep-ph/9610336](#).
J. Berges, D.U. Jungnickel, and C. Wetterich, Phys. Rev. **D59** (1999), 34010.
K-I. Aoki, K. Morikawa, J-I. Sumi, H. Terao and M. Tomoyose, Prog. Theor. Phys. **97** (1997), 479; KANAZAWA-99-11, KUCP-0139, [hep-th/9908042](#).
- 2) K-I. Aoki, K. Morikawa, J-I. Sumi, H. Terao and M. Tomoyose, KANAZAWA-99-12, KUCP-0140, [hep-th/9908043](#).
- 3) M. Alford, Phys. Lett. **B336** (1994), 237.
N. Tetradis and C. Wetterich, Nucl. Phys. **B422** (1994), 541.
K-I. Aoki, K. Morikawa, W. Souma, J-I. Sumi and H. Terao, Prog. Theor. Phys. **95** (1996), 409; **99** (1998), 451.
- 4) Y. Nambu and G. Jona-Lasinio, Phys. Rev. **122** (1961), 345.
- 5) D. Gross and A. Neveu, Phys. Rev. **D10** (1974), 3235
- 6) Y. Iwasaki, Nucl.Phys.B (Proc. Suppl.) **42** (1995)96.
K. Kanaya, Nucl.Phys.B (Proc. Suppl.) **47** (1996)144.
A. Ukawa, Nucl.Phys.B (Proc. Suppl.) **53** (1997)106.
S. Aoki, A. Ukawa and T. Umemura, Phys. Rev. Lett. **76** (1996), 873.
- 7) I. Barbour, C. Davies and Z. Sabeur, Phys. Lett. **B215** (1988), 567.
I. Barbour, S. Morrison, E. Klepfish, J. Kogut, M. -P. Lombardo, Nucl.PhysA (Proc. Suppl.) **60** (1998)220.
- 8) E. Dagotto, A. Moreo, R. Sugar, D. Toussaint, Phys. Rev. **B41** (1990), 811.
N. Weiss, Phys. Rev. **B35** (1987), 2495.
A. Hasenfratz and D. Toussaint, Nucl. Phys. **B371** (1992), 539.
M. Alford, A. Kapustin, F. Wilczek, Phys. Rev. **D59** (1999), 54502.
- 9) A. Hasenfratz and P. Hasenfratz, Nucl. Phys. **B270** (1986), 269.
- 10) K.G. Wilson, I.G. Kogut, Phys. Rep. **12** (1974), 75.
- 11) F. Wegner, A. Houghton, Phys. Rev. **A8** (1973) 401.

J. Polchinski, Nucl. Phys. **B231** (1984), 269.

A. Hasenfratz, P. Hasenfratz, Nucl. Phys. **B270** (1986), 685.

G. Keller, C. Kopper and M. Salmhofer, Helv. Phys. Acta **65** (1992), 32.

12) C. Wetterich, Phys. Lett. **B301** (1993), 90.

M. Bonini, M. D'Attanasio, and G. Marchesini, Nucl. Phys. **B409** (1993), 441.

13) C. Wetterich, Z. Phys. **C57** (1993), 451.

N. Tetradis and C. Wetterich, Nucl. Phys. **B422** (1994), 541.

T.R. Morris, Phys. Lett. **B329** (1994), 241.

14) T. Inagaki, T. Kouno and T. Muta, Int. J. Mod. Phys. **A10** (1995), 2241.

15) D. O'Connor and C. R. Stephens, Phys. Rev. Lett. **72** (1994), 506; Int. J. Mod. Phys. **A9** (1994), 2805.

16) S. Coleman, Commun. Math. Phys. **31** (1973), 259.

E. Witten, Nucl. Phys. **B145** (1978), 110.

17) J. Conwarll, R. Jackiw and E. Tomboulis, Phys. Rev. **D10** (1974), 2428.

18) M. Inoue, H. Katata, T. Muta and K. Shimizu, Prog. Theor. Phys. **70** (1988), 519.

19) T. R. Morris, Int. J. Mod. Phys. **A9** (1994), 2411; Nucl. Phys. **B458** (1996), 477.

20) J. Berges, D.-W. Jungnickel and C. Wetterich, MIT-CTP-2794, HD-THEP-98-57, [hep-ph/9811347](#).

21) L. Dolan and R. Jackiw, Phys. Rev. **D9** (1974), 3320.

P. Arnold and O. Espinosa, Phys. Rev. **D47** (1993), 3546.

22) For Crank-Nicholson method and the trapezoidal rule, see for example, W. H. Press, S. A. Teukolsky and W. T. Vetterling, B.P. Flannery, *Numerical Recipes in FORTRAN* (Cambridge Univ. Press, 1994).

23) K. Ogure and J. Sato, Phys. Rev. **D57** (1998), 7460.

24) G. 'tHooft, Phys. Rev. **D14** (1976), 3432.

25) R. Fukuda, Prog. Theor. Phys. **56** (1976), 258.

L. O'raifeartaigh, A. Wipf and H. Yoneyama, Nucl. Phys. **B271** (1986), 653.

26) S. Seide and C. Wetterich, HD-THEP-98-20, [cond-mat/9806372](#).

N. Tetradis and C. Wetterich, Nucl. Phys. **B383** (1992), 197.

A. Ringwald and C. Wetterich, Nucl. Phys. **B334** (1990), 506.

J. Alexandre, V. Branchina and J. Polonyi, [cond-mat/9803007](#).

27) D. Baillie and A. Love, Phys. Rep. **107** (1984), 325.

M. Iwasaki and T. Iwado, Phys. Lett. **B350** (1995), 163.

R. Rapp, T. Schaefer, E. V. Shuryak and M. Velkovsky, Phys. Rev. Lett. **81** (1998), 53.

M. Alford, K. Rajagopal and F. Wilczek, Nucl. Phys. **B537** (1999), 443; **B537**

(1999), 443; **A638** (1998), 515c; Phys. Lett. **B422** (1998), 247.
N. Evans, J. Hormuzdiar, S. Hsu and M. Schwetz, BUHEP-99-25, [hep-ph/9910313](#)
S. Hsu and M. Schwetz, Phys. Lett. **B432** (1998), 203; OITS-676, [hep-ph/9908310](#).
N. Evans, S. Hsu and M. Schwetz, Phys. Lett. **B449** (1999), 281; Nucl. Phys. **B551**
(1999), 275.
M. Alford, J. Berges and K. Rajagopal, MIT-CTP-290, [hep-ph/9910254](#); MIT-CTP-
2889, [hep-ph/9908235](#); MIT-CTP, [hep-ph/9903502](#).
J. Berges, MIT-CTP-2829, [hep-ph/9902419](#).
J. Berges and K. Rajagopal, Nucl. Phys. **B538** (1999), 215.